



# Mechanical behavior of reactive air brazed (RAB) Crofer 22 APU-Al<sub>2</sub>O<sub>3</sub> joints at ambient temperature

Wolfgang Tillmann<sup>1</sup> · Nadeem Babar Anar<sup>2</sup> · Lukas Wojarski<sup>1</sup>Received: 12 February 2020 / Accepted: 26 March 2020 / Published online: 3 April 2020  
© Springer Nature Switzerland AG 2020

## Abstract

The evolution of innovative high-temperature electrochemical devices, such as high temperature solid oxide fuel cells (SOFCs), gas separators and gas reformers, consisting of metal–ceramic-joints is challenging. The seals have to be stable and gastight in isothermal high-temperature as well as in thermo-cyclic operation. Here, the reduction of porosity is the primary aim, to obtain air brazed joints with a long lifetime. In the last years, reactive air brazing (RAB) has gained rising interest for the joining of ceramic–ceramic and ceramic–metal compounds. In this paper an alternative brazing filler metal manufacturing process employing (physical vapor deposition (PVD)) is applied and its feasibility for the production of metal–ceramic composites has been investigated for Ag–4 wt%CuO. For RAB aluminum oxide with ferritic high chromium steel Crofer22APU have been joined. The pore formation in subordination of the braze and base materials can be monitored after brazing. By modifying the brazing process, the pore formation in the joints can be avoided. The microstructure of brazed joints with the developed braze foils is studied. Discussion of the results focuses on the influence of microstructural evolution on mechanical properties, the pore formation in the brazing seam and failure behavior of the brazed joints. A correlation between the process parameters brazing temperature and holding time and the achieved compound properties could be derived. Further, excellent wetting of the ceramic was obtained. The highest shear strength with 123 MPa was measured for a temperature of 1000 °C and 5 min, using the Ag4CuO alloy.

**Keywords** Reactive air brazing (RAB) · Physical vapor deposition (PVD) · Metal–ceramic composites · Microstructure · Shear strength · Fracture

## 1 Introduction

Ceramic–metal compounds are becoming increasingly important for a large number of technical applications [1]. High-temperature heat exchangers, gas turbines and combustion engines are examples of such advanced power generation devices. There is a growing demand to generate materials appropriate for the industrial use, especially for the operation under oxidizing conditions [2, 3]. Ceramics offer totally new capabilities due to their exceptional high-temperature material properties. These enables their

usage for many high-temperature technology [4, 5]. The fabrication of ceramic–metal compounds allows to combine the mechanical properties of these material classes. However, the joining of ceramics to themselves or to a metallic counterpart is a challenging task by reason of the insufficient wetting behavior of metallic filler brazes on ceramics [6]. The brazing process for these applications induces high internal thermal stresses during cooling due to large differences in the coefficients of the thermal expansion (CTE) [7]. Moreover, due to different chemical

✉ Nadeem Babar Anar, nadeem.anar@rif-ev.de; Wolfgang Tillmann, wolfgang.tillmann@udo.edu; Lukas Wojarski, lukas.wojarski@udo.edu | <sup>1</sup>Institute of Materials Engineering, TU Dortmund University, Leonhard–Euler–Str. 2, 44227 Dortmund, Germany. <sup>2</sup>RIF Institute for Research and Transfer e.V., Joseph–von–Fraunhofer–Straße 20, 44227 Dortmund, Germany.



bonds in metals and ceramics molten metals do not wet ceramic surfaces and a direct brazing is not feasible [8, 9].

Furthermore, there exist a variety of joining methods to join ceramic–metal composites. The most common and well known direct joining technology is active brazing with metallic filler materials [6, 10–12]. Thereby up to 10 mol% of interfacial active elements such as titanium, hafnium, chromium, or zirconium are added to the braze filler metal. These elements react with the ceramic joining partner to form an adhesion promoting layer. New phases or reaction layers are formed at the interface which have a metallic or metal-like structure [6]. The modified chemical bonds causes a strong reduction of the surface tension, so that the reaction layer can be wetted by the active filler metal [9]. The active brazing process has been used very effectively for decades in the industry and a variety of commercial active filler brazes are available. Certainly, active brazing can only be carried out under high vacuum or in an inert protective atmosphere with very low oxygen partial pressures [9, 13, 14]. Some functional ceramics, like cathode materials used for example for solid oxide fuel cells (SOFCs), are not stable in these atmospheres [15]. Additionally, experimental works have demonstrated that the active brazed joints are unreliable at temperatures above 500 °C, whereupon they ultimately oxidize entirely, conferring minimal or neglectable bonding to the produced joints [16–18].

Another alternative well-known joining procedure is the brazing of metallized ceramics. This process involves a Mo–Mn metallization and following Ni plating of the ceramic surfaces prior to brazing. However, these two joining techniques are complex and expensive because of extended process costs compared to air-fired processes. Further, the joining methods described above require a lot of practical experience [10, 19]. Furthermore, glass joining is a quite easy but certainly costly technique of bonding ceramic materials. But the maximum operating temperature of a glass joint is restricted by the softening point of the glass utilized. Moreover glass devitrification occurs during use because the glass changes its thermomechanical properties from the initial state [2, 20]. Another joining process for ceramics is diffusion bonding. Thereby high temperatures and high pressures are needed. Certainly, due to the high pressure demand, components produced by diffusion bonding are generally restricted to simple geometry [2, 21].

Therefore, in the past 20 years, a new ceramic–ceramic and ceramic–metal joining technique publicized as reactive air brazing (RAB) has been explored exceedingly for high-temperature applications [2, 3, 22–26]. In numerous points, RAB is alike to active metal brazing process [9, 13]. RAB process is realized in air atmosphere and the respective joints show impervious high temperature oxidation

behavior. Reactive air brazing can be conducted without the consumption of fluxing or reducing agents to support wetting [18]. Based on, direct copper bonding, which is the origin of RAB, Kim et al. [2] and Weil et al. [24, 27] established this joining method experimenting with a silver-copper oxide (AgCuO) braze, on be brazed in an air atmosphere [28].

The principle of RAB is to use a molten oxide (commonly copper) dissolved in a noble metal solvent (commonly silver) to prewet the ceramic surfaces, in this way shaping a new surface that is more wettable by the remaining molten filler braze metal [3, 29]. The wetting of ceramics is possible due to in situ formed oxides in the melted braze during the brazing process [29]. The wetting of the ceramic is caused by the partial miscibility gap of the AgCuO-system [29–32]. The emerging joint is well adherent, ductile, and basically oxidation resistant [3, 18]. The bonding strength depends on the copper oxide content and the formed reaction layers at the different material interfaces [2, 23, 27]. Chen et al. [26] analyzed the wetting mechanisms of some common ceramic–metal compounds by RAB using Ag–Cu brazing alloys. The authors have shown that the produced joints are hermetic and stable to thermal aging (750–950 °C).

However, while joining ceramics to metals with Ag–Cu-based RAB filler metals, an often outlined problem is the reaction between the braze alloy and the metal. Thick interfacial reaction layers, which can be identified on the surface of all commonly used steels, will cause brittleness in the joint as well as a reduced long-term reliability [8, 33, 34]. A further detriment of RAB is that the brazed joints frequently hold a distinct porosity conducting to a low tightness and corrosion resistance along with a reduced strength [35]. These obstacles still limit the use of RAB in industrial applications [36]. One conceivable solution for the formation of the reaction layer is to control the reactions between the braze filler alloy and the base metal during the brazing process [8, 34]. Furthermore, the high joining temperature of approximately 1000 °C and brazing in air ensure that only high-temperature resistant metallic materials are appropriate for the use as base materials for RAB [33, 36].

To achieve optimal joint characteristics in RAB, it is important to determine optimal brazing temperatures and holding times. Researching the optimal brazing parameters may offer the use of RAB as an alternative for a large number of practical industrial applications. Up to now, only some studies have recommended optimized reactive brazing parameters.

Most of the published articles refer to the RAB of yttria-stabilized zirconia (YSZ) with ferritic high chromium steel Crofer 22 APU [30, 33, 37, 38], approaches to increase the shear strength of reactive air brazed aluminum oxide

**Table 1** Chemical composition (wt%) of Crofer 22 APU (1.4760) X1CrTiLa22 [8, 39]

Fe	Cr	Mn	Ti	La	Si	C
Bal.	20–24	0.3–0.8	0.03–0.2	0.04–0.2	< 0.5	< 0.03

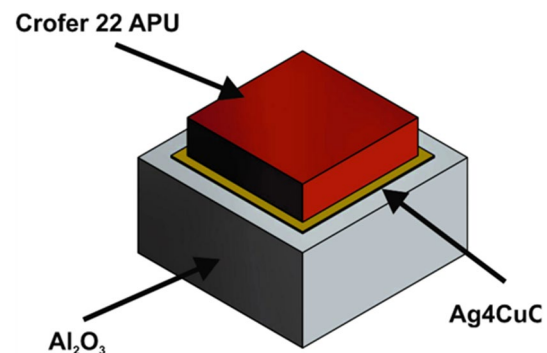
(Al<sub>2</sub>O<sub>3</sub>) and Crofer 22 APU joints with a silver-copper oxide (Ag<sub>4</sub>CuO) brazefoil are not yet thoroughly investigated. Thus, a brazing filler manufacturing process including arc-PVD coating of copper on both sides employing a pure silver foil will be analyzed for the production of metal–ceramic composites. In addition, it will be examined how the copper layer affects the adhesion to the ceramic and steel. Also, the pore formation will be investigated after the brazing process due to the melting and wetting progression and a reaction between the braze and the base materials. Finally, the microstructure of brazed joints, the influence of microstructural evolution on mechanical properties, the pore formation in the brazing seam and failure behavior of the brazed joints will be discussed.

## 2 Materials and methods

### 2.1 Materials

In this study, all experiments were executed utilizing the ferritic high chromium steel VDM® Crofer 22 APU (1.4760, X1CrTiLa22, UNS S4 4535) as the metallic base material. This high-temperature ferritic steel was developed by ThyssenKrupp VDM GmbH under licence from Forschungszentrum Jülich particularly for the application in SOFCs [39]. It was especially designed as a common interconnect material for SOFCs [40]. The thermal expansion was accommodated to that of ceramics inserted for industrial high-temperature electrochemistry uses e.g. fuel cells in the interval from room temperature to 900 °C [39]. The coefficient of thermal expansion (CTE) of this steel in the range from 20 to 1000 °C is  $12.7 \times 10^{-6} \text{ K}^{-1}$ . Furthermore, corrosion and electrical resistance experiments in air and reducing atmospheres have proven, that the formation of a chromium-manganese oxide layer is formed on the surface of Crofer 22 APU. This formed oxide layer contains of a fine grained inner scale Cr<sub>2</sub>O<sub>3</sub> and a columnar (Mn, Cr)<sub>3</sub>O<sub>4</sub> spinel outer oxide layer. The outer oxide layer reduces chromium evaporation very successfully. The chromium-manganese oxide layer is thermodynamically very stable and courses high electrical conductivity [39, 41–44]. The chemical composition of the Crofer 22 APU is summarized in Table 1. The steel samples were cut into 7 mm × 7 mm × 2 mm coupons and grinded with a 1200 grid silicon carbide abrasive grinding paper.

As the ceramic joining partner aluminum oxide Al<sub>2</sub>O<sub>3</sub> (Degussit ceramic AL23, Kyocera Fineceramics Solution

**Fig. 1** Schematic arrangement of Crofer 22 APU and Al<sub>2</sub>O<sub>3</sub> for the joining process**Table 2** Structure and chemical composition (wt%) of the AgCu-brazing foil

Type of coating	Ag-foil (μm)	Cu coating (μm)	Chemical composition
On both sides	76	2.5	Ag <sub>4</sub> Cu

GmbH, Mannheim, Germany) was used as base material in this work. The CTE of this ceramic in the range from 20 to 1000 °C is  $8.2 \times 10^{-6} \text{ K}^{-1}$  [45]. The ceramics were supplied as rectangular plates measuring 100 mm long × 50 mm wide × 4 mm thick and featured purity of > 99.5 wt%. The ceramic parts to be joined were cut into shape of squares (10 mm × 10 mm). The samples were applied in the as fired state without any additional processing of the surface. Subsequently, steel and ceramic base materials were cleaned with ethanol in an ultrasonic bath for 15 min immediately before joining. The assembled steel and ceramic parts during the joining process are shown schematically in Fig. 1.

For all joining experiments in this study, a silver-based RAB-alloy with small amount of CuO was used. The RAB-foils Ag<sub>4</sub>Cu (wt %) were manufactured by arc-(physical vapor deposition (PVD)) coating process. The AgCu-foils consisted of a 76 μm thick pure silver foil (25.4 mm wide, 99.99% Ag) on which a thin layer of copper was deposited by arc-PVD on both sides, which corresponds to the ratio of the desired composition of the braze foil (cf. Table 2). The concentration of Ag<sub>4</sub>Cu is reached by a defined thickness of the copper layer. The braze foils were positioned between the joining components (see Fig. 1). The copper oxide was then formed in situ during the brazing process

in the furnace, whereby the copper reacted with the ambient atmosphere of the air furnace to form copper oxide (CuO).

## 2.2 Arc-PVD coating

Prior to the arc-PVD coating deposition of copper, pure Ag-foils were cleaned for 15 min in an ultrasonic ethanol bath. After drying in heated air the foils were positioned in the arc-PVD device (Arc-PVD20, Sulzer Metaplas GmbH, Germany). A commonly used arc-PVD process was chosen to apply a thin copper layer film on both sides of the Ag-foil [46–48]. The coating process consisted of two different steps. Prior to the coating process, a short plasma-etching process was realized under vacuum with a bias voltage of  $-1$  kV without surpassing a maximum temperature of  $350$  °C. During this process, high energized target ions are accelerated onto the surface of the foils because of a high bias voltage and remove oxides and pollutants from the substrate surface. The etching process activates the surface and increases the adherence between the silver foil and the copper layer [49]. For the final coating process, a bias voltage of  $-36$  V and a current of  $70$  A were adjusted to deposit pure copper thin films with an average thickness of  $2.5$   $\mu\text{m}$ . An electrical charge of  $90$  Ah was conducted to manufacture the braze filler metal. Meanwhile the temperature of the foils was controlled to a maximum of  $350$  °C. The cross-section morphology of the silver foil after arc-PVD coating is shown in Fig. 2.

A layer of compact copper continuously formed on both sides of the foil. The thickness of the deposited copper layer was almost homogeneous. Individual small droplets were formed during the coating process. The thickness of the copper layer was increased by varying the deposition rate. However, the subsequent brazing process was not affected by this.

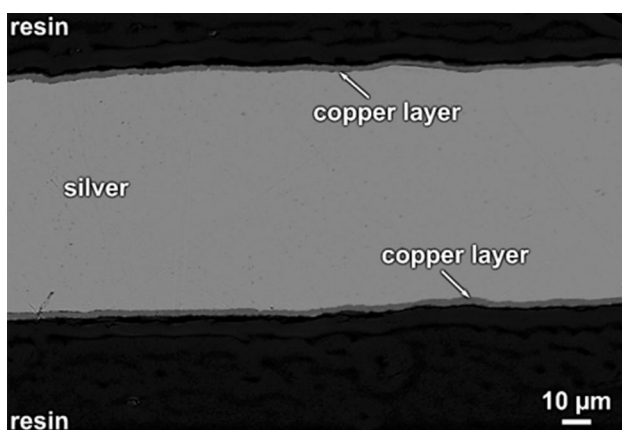


**Fig. 2** Cross-section morphology of the brazing foil after arc-PVD coating

## 2.3 RAB procedure

The braze filler metal was applied in form of a foil and positioned between the ceramic and steel. This assembly was placed upright in an air furnace (Nabertherm N100, Lilienthal, Germany). Three different commonly used brazing temperatures ( $1000$  °C,  $1050$  °C and  $1100$  °C) were used with three different dwell times ( $5$  min,  $15$  min and  $30$  min). Short brazing times of  $5$  min were chosen to minimize the diffusion process and the formation of brittle phases and reaction layer at the Crofer/braze filler metal interface. The heating rate of the brazing cycle was about  $5$  K  $\text{min}^{-1}$ . At  $500$  °C, an intermediate holding time of  $30$  min was used to form in situ oxidation of the copper to copper oxide (CuO) and to ensure a homogenous temperature distribution. Subsequently, the temperature was further increased with  $5$  K  $\text{min}^{-1}$  to the desired brazing temperature. After the holding time at the maximum brazing temperature, uncontrolled cooling of the furnace was performed to ambient temperature.

The process temperature was controlled with type K thermocouple according to the core temperature of a reference sample with same geometry and identical materials, during brazing. This sample was positioned in the middle of the furnace. Figure 3 visualized an exemplary course of a time–temperature-curve for the conducted RAB experiments. The comparison of the target temperature profile with the measured temperature profile shows only minor deviations from the measured temperature behavior of the samples from the default values. The tolerances are determined by the inertia of the air furnace itself, the samples and the position of the thermocouple. A total of five specimens were brazed per parameter set.

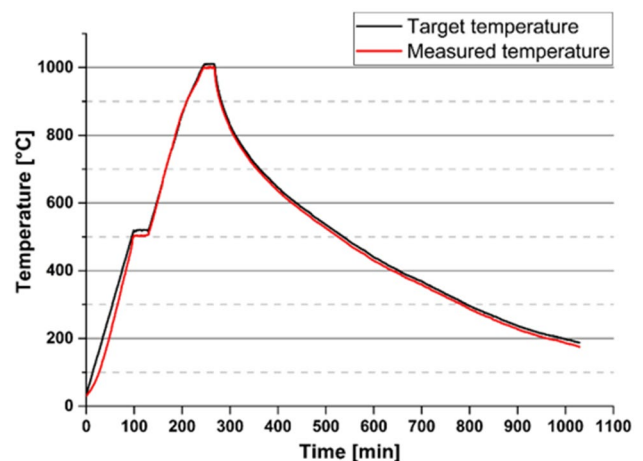


**Fig. 3** Exemplary time–temperature-curve for the conducted RAB experiment ( $T_b = 1000$  °C,  $t_d = 30$  min)



## 2.4 Microstructural and mechanical analyses

The investigations of the microstructure of the brazed joints and the fractography of the specimens was conducted using the field emission scanning electron microscope (SEM) (FE-JSEM 7001F, Jeol, Japan). Therefore, specimen cross-sections of the brazed joints were embedded utilizing metallographic preparation techniques. A 3D-digital microscope (DVM6, Leica microsystems GmbH, Wetzlar, Germany) was used to analyze the morphology and to determine the porosity of the specimen cross-sections. Additionally, qualitative and quantitative elemental analyses were accomplished using energy dispersive X-ray spectroscopy (EDS) employing the EDS detector from Oxford Instruments and the software INCA. EDS point scans were utilized to analyse local sample chemical compositions. Different SEM images of the specimens were taken employing the secondary electron (SE) detector and a backscattered electron (BSE) detector. All analyses were realized at an acceleration voltage of 20 kV. Additional measurements of microstructural hardness (Vickers HV 0.01) were performed using the Duramin-40 A1 testing machine.

The shear strength of the brazed joints was measured at room temperature, using the hydraulic universal testing machine (Mohr & Federhaff, Germany). The brazed specimens were sheared using a special set-up according to the schematic drawing shown in Fig. 4.

The coupon was placed between the two fixations on the shear device and therefore can only be moved in loading direction. These fixations over the apparatus hold the joining components and guarantees an evenly distributed force induction. The placement of the specimen was scheduled to keep friction and bending stress

to a minimum. The position of the steel was fixed by the shearing edge of the device, the ceramic counterpart was pressed through the slot in the apparatus, which was adjusted according to the dimensions of the  $\text{Al}_2\text{O}_3$  coupon. The bottom of the aluminum oxide is free in movement, so the ceramic can be sheared through the gap in the device. The applied force was increased until the brazing joint failed and the steel part was sheared off. The ultimate shear strength of the joints was considered as the mean value of the quotient of the maximum measured force and the wetted shear area. In order to determine the wetted area a 3D-digital microscope (DVM6, Leica) was used employing the processing software called LAS X. Per brazing parameter variation an average of four specimens were prepared for the shear strength experiments.

## 3 Results and discussions

### 3.1 Microstructural characterisation

The microstructures of reactive air brazed Crofer 22 APU- $\text{Al}_2\text{O}_3$  joints using Ag4CuO filler alloy at 1000 °C for a holding time of 5 and 30 min are shown in Figs. 5 and 6.

The cross-sectional backscattered electron images show that brazing at 1000 °C for 5 and 30 min were adequate to produce pore and void-free uniform brazed joints. Through the outstanding wetting behavior of the molten braze foil, a tight linking to the aluminum oxide and to the ferritic high chromium steel could be observed. Both interfaces of the steel and the ceramic component of the brazing seam were continuous and free of cracks. Even if CuO and Ag form a liquid solution

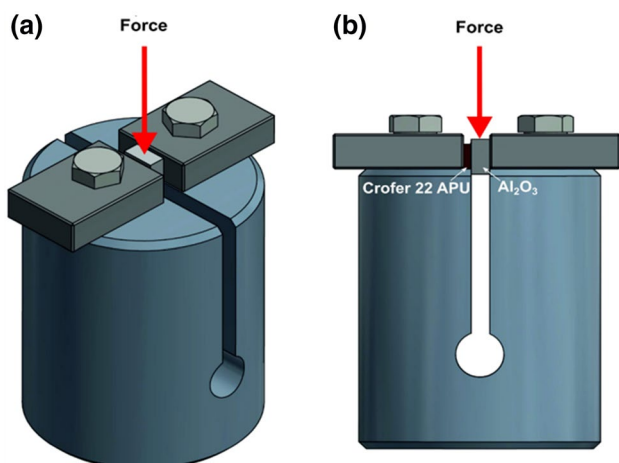


**Fig. 4** **a** Schematic illustration of the shear experiment device, **b** for a better visualization side view of the test device

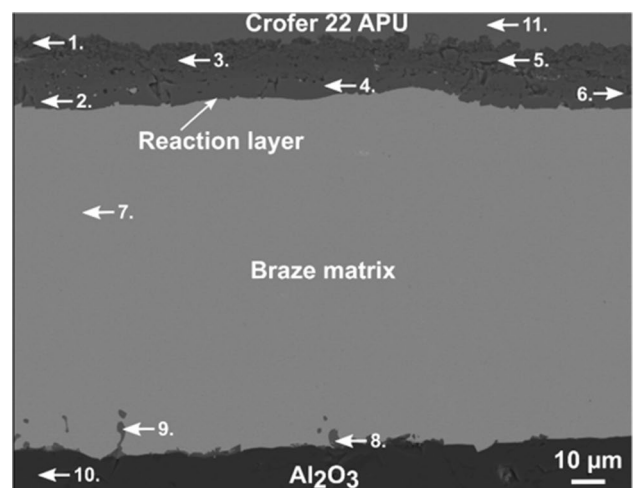


**Fig. 5** Cross-sectional backscattered SEM micrograph of a Crofer 22 APU- $\text{Al}_2\text{O}_3$  joint brazed using the Ag-4CuO filler alloy ( $T_b = 1000$  °C,  $t_d = 30$  min)

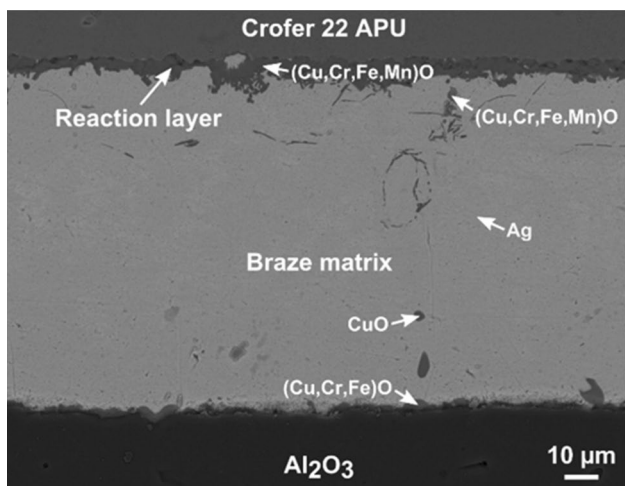


**Fig. 6** Cross-sectional backscattered SEM image of a Crofer 22 APU-Al<sub>2</sub>O<sub>3</sub> joint brazed using the Ag-4CuO filler alloy ( $T_b = 1000\text{ }^\circ\text{C}$ ,  $t_d = 5\text{ min}$ )



**Fig. 7** Digital microscope overview of the complete RAB joint area ( $T_b = 1000\text{ }^\circ\text{C}$ ,  $t_d = 5\text{ min}$ )

during the melting process, CuO is prone to precipitate during cooling due to the reduced solubility limit [50]. The development of a consistent brazing zone proved that the Ag4CuO braze filler metal wetted the components satisfactory through a liquid–solid interaction through RAB process. Figure 7 show an exemplary digital microscope overview of the complete joint area, which is representative for the brazed joints.

The joints in Figs. 5 and 6 are essentially consisted of three different zones: the brazing filler metal–aluminum oxide interface (Ag4CuO-Al<sub>2</sub>O<sub>3</sub>), the central brazing seam zones composed of the braze components and diffusion elements from Crofer and the reaction layer at the Crofer-brazing filler metal interface (Crofer–Ag4CuO). The Crofer-brazing filler metal interface is the most significant interfacial zone. The SEM-analysis together with appropriate EDS-analysis and microhardness measurements allows a closer evaluation of the resulting microstructure.

A dense reaction layer at the interface between Crofer and the braze filler metal is visible in Fig. 5. The thickness of the reaction layer is about 18–20 µm. These reaction layer is visualized as a black area in the SEM image in Fig. 5. The reaction layer consists of different phases, which were revealed by EDS-analyses. The complete chemical compositions are given in Table 3. The reaction layer mainly consists of a mixed oxide, including primarily chromium, iron and copper with small amounts of manganese (localization 2, 4 and 6) what is in sound accordance to the literature [33, 51, 52]. Some segregated iron-rich mixed oxides (Cu–Fe–Cr–O) can be observed (localization 3 and 5) in the reaction layer. The existence of Cu in the reaction layer displays that Cu diffuses from the braze matrix into the reaction layer. In adherence to the steel, high content of chromium was found in position 1. The mixed oxides Cu/Cr/Fe/Mn were molded through the reaction of the CuO-containing silver braze filler metal with the steel surface during the heating process. Therefore, the reaction layer was shaped by the oxidation of Fe, Cr and Mn that diffuses out from the Crofer and the diffusion of CuO from the braze filler metal into this reaction layer. Consequently, the formation of the reaction layer on the steel side is inevitable when RAB is employed [50]. Related results in the literature prove the preferential formation of Cr<sub>2</sub>O<sub>3</sub> at the surface of Crofer 22 APU due to the superficial diffusion of Cr at the brazing temperatures [44, 53]. Furthermore

**Table 3** Chemical composition of the microstructure of Fig. 5

Pos.	Chemical compositions (wt %)						
	Ag	Cu	Fe	Cr	Mn	Al	O
1			32.72	31.77			35.51
2		23.83	43.48	3.55	1.05		28.08
3		10.22	28.91	27.43			33.44
4		23.41	41.62	5.29	1.42		28.27
5		6.57	33.78	30.45			39.20
6		7.91	57.47	5.16	0.69		28.77
7	100.0						
8		56.59	2.90	4.66			35.85
9		75.40					24.60
10						49.92	50.08
11			79.25	20.75			

$\text{MnCr}_3\text{O}_4$ ,  $\text{CuCr}_2\text{O}_4$  and  $\text{FeCr}_2\text{O}_4$  spinel oxides moulded by a reaction between  $\text{Cr}_2\text{O}_3$  and  $\text{Mn}_3\text{O}_4$ ,  $\text{CuO}$  and  $\text{Fe}_2\text{O}_3$  appropriately during the RAB [54].

However, the braze- $\text{Al}_2\text{O}_3$  interfaces are not strongly influenced by the different holding times (5 and 30 min) during the brazing processes at  $1000^\circ\text{C}$  and show comparable microstructures (see Figs. 5, 6). There were no reaction layers traceable at the braze- $\text{Al}_2\text{O}_3$  interface. EDS-analysis proved that the joint gap is filled with pure silver and can be recognized as a grey area in position 7 (Fig. 5). In the Ag braze filler metal matrix solid inclusions of copper oxide with small amount of chromium and iron are randomly distributed and appear as a dark grey area (localization 8). At the interface braze- $\text{Al}_2\text{O}_3$  only minor segments of precipitated pure  $\text{CuO}$  particles are visible (localization 9), as shown in the magnified image in Fig. 5. However, in the complete Ag-rich brazing seam no  $\text{CuO}$  particles could be detected. The silver remained well-bonded to the aluminum oxide. At the braze filler metal- $\text{Al}_2\text{O}_3$  interface, the Ag4CuO braze demonstrates outstanding adhesion behavior to aluminum oxide in RAB. The interfacial adhesion at the ceramic interface specifies the presence of very solid atomic bonds [55]. Coating of copper by arc-PVD on the surface of pure silver foil demonstrates to be prosperous in this study. Copper appears to have an appropriate reactivity with the oxygen, developing a thick reaction layer at the braze filler metal-Crofer interface.

The digest of the joint brazed at  $1000^\circ\text{C}$  for 5 min along with the braze- $\text{Al}_2\text{O}_3$  interface and Crofer-braze filler metal interface at exalted magnification is shown in Fig. 6. The cross-sectional SEM image shows a perfect blend, without any defects and pores. Furthermore, the interfaces are crack free and a sound joining was succeeded. The reaction layer detected at the Crofer interface is also visible in Fig. 6. The thickness of the reaction layer is about  $5\text{--}7\ \mu\text{m}$  and appears as well as a light black area in the SEM image. The silver also is well-bonded to the aluminum oxide surface. The essential difference between the brazed joints is that with decreasing holding time from 30 to 5 min at a fixed temperature of  $1000^\circ\text{C}$ , less of the reaction layer is formed. This aspect may have an enormous influence on the shear strength test results.

The development of the reaction layer on the Crofer surface is problematical for prospective industrial applications as described above in this work. This reaction layer is alleged to have inappropriate mechanical properties. Microhardness measurements exposed that the extremely hard one mixed oxide layer exposed a very brittle behavior. The microhardness indents formed small cracks in the reaction layer (see Fig. 8b). Regarding the composition of this reaction layer, the high volume of chromium, iron and oxygen in connection with copper is responsible for its high microhardness. A microhardness of 580 HV0.01

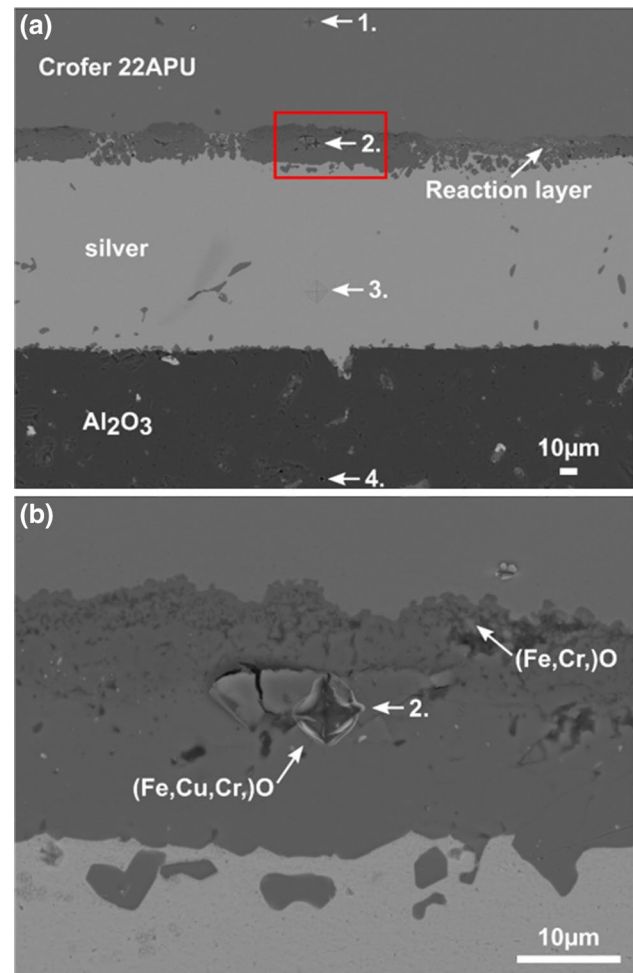


**Fig. 8** **a** Microhardness indents (HV0.01) at different selected positions of a Crofer 22 APU- $\text{Al}_2\text{O}_3$  joint brazed with Ag-4CuO filler alloy ( $T_b = 1000^\circ\text{C}$ ,  $t_d = 30\ \text{min}$ ), **b** microhardness indent in the reaction layer and resulted cracks

was determined at position 2. It is much greater than the microhardness of the Ag braze matrix (90 HV0.01) at position 3 in Fig. 8a. For a better comparison, the microhardness after the brazing process of the Crofer 22 APU (245 HV0.01) at position 1 and the  $\text{Al}_2\text{O}_3$  (2650 HV0.01) at position 4 was determined.

### 3.2 Shear strength properties

The shear strength results of the reactive air brazed components depend on the microstructure and the interface reactions between the braze filler metal with the joining steel and ceramic partners. In Fig. 9, the average shear strength values of the reactive air brazed Crofer 22 APU- $\text{Al}_2\text{O}_3$  samples using the Ag-4CuO filler alloy for three different brazing temperatures ( $1000^\circ\text{C}$ ,  $1050^\circ\text{C}$

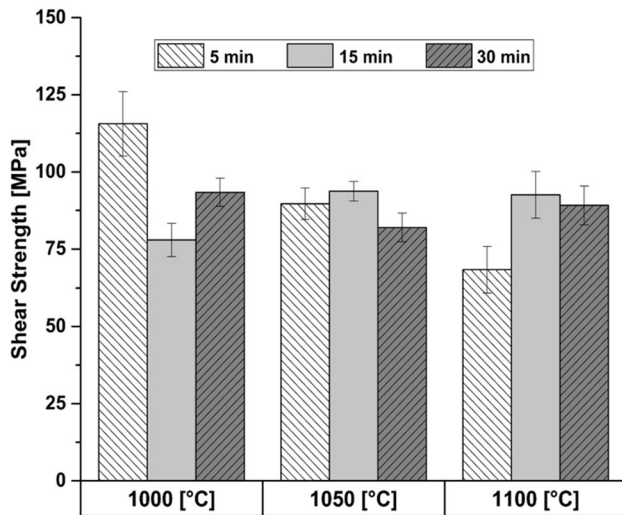


**Fig. 9** Comparison of the shear strength of reactive air brazed Crofer 22 APU- $\text{Al}_2\text{O}_3$  samples using the Ag-4CuO filler alloy and different brazing parameters

and 1100 °C) and three different holding times (5 min, 15 min and 30 min) are shown together with the standard deviation.

As can be seen in the diagram, the standard deviations for the different brazing parameters are very low. Generally, as the brazing temperature increases obviously from 1000 to 1050 °C for a holding time of 5 min, average shear strength decreases from  $115 \pm 10$  MPa to  $89 \pm 5$  MPa. After increasing the brazing temperature at the same holding time to 1100 °C, the shear strength decreases substantially to  $68 \pm 7$  MPa. As the brazing temperature increases from 1000 to 1050 °C for a dwell time of 30 min, the average shear strength decreases from  $93 \pm 4$  MPa to  $82 \pm 4$  MPa. A brazing temperature of 1100 °C for 30 min dwell time results in a marginally increase to  $89 \pm 5$  MPa.

In the shear experiments the highest shear strength of 123 MPa was achieved for temperature of 1000 °C and a holding time of 5 min. The lowest shear strength of 62 MPa for a brazing temperature of 1100 °C and a holding time of 5 min was obtained. However, as shown in Fig. 9 the influence of the different brazing temperatures at a holding time of 5 min is more pronounced than at 15 and 30 min. Further, increasing holding times from 15 to 30 min at brazing temperatures of 1050 °C and 1100 °C decreases the shear strengths. This perhaps caused by the development and formation of the reaction layer at the Crofer 22 APU-braze filler metal interface. The shear strength experiment results will be directly correlated to the fracture mechanisms and fracture surfaces in the next section of this paper.

### 3.3 Fractography analysis

To approve these declarations and the prospect to differentiate between the microstructural and shear strength properties appearance and failure mechanisms of the reactive air brazed joints, fracture investigations with the SEM and 3D-digital microscope was accompanied for the fracture surfaces and at the different cross-sections of the specimens.

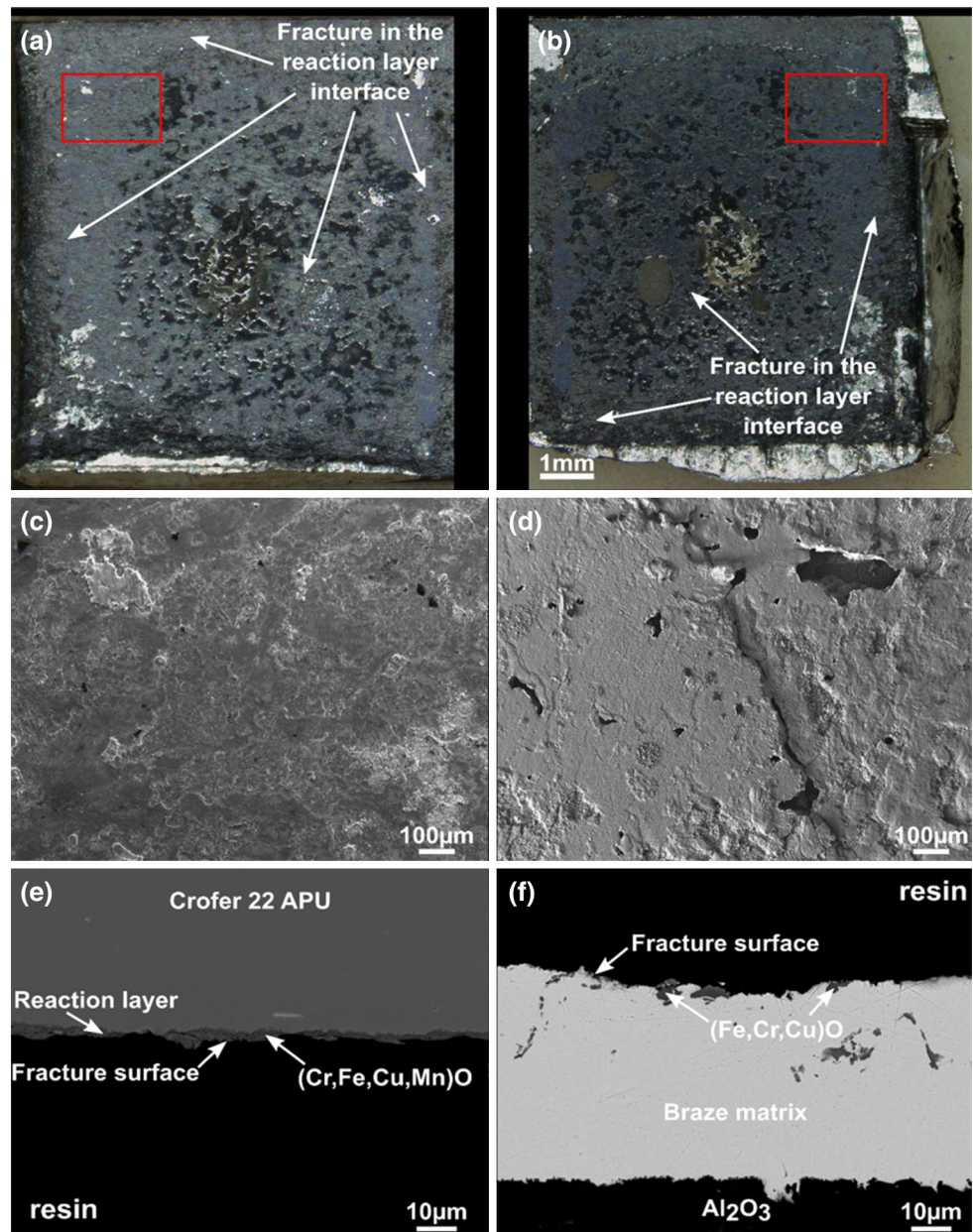
Figure 10a and b depict the digital microscope images of two corresponding halves of fractured reactive air brazed Crofer 22 APU/Ag4CuO/ $\text{Al}_2\text{O}_3$  components brazed at 1000 °C for 5 min after the shear strength test. As visible in the images the Crofer and the aluminum oxide side of the specimens reveal the surfaces covered by the oxide elements of the reaction layer with very small dots of silver. The SEM micrographs show the cross-sections of the Crofer (see Fig. 10e) and the  $\text{Al}_2\text{O}_3$  (see Fig. 10f) after fracture. The failure in the shear test was perceived to be controlled by interfacial phenomena.

The fracture is noticeable within the interfacial reaction layer at the braze filler metal–Crofer interlayer. The mixed oxides contain chromium, iron and copper with small amounts of manganese. This reaction layer is very brittle due to its high microhardness as previously described in this work. The fracture investigation highlighted the critical function of brittle oxide layers shaped on the Crofer surface as reaction products during the brazing process. The mechanical failure favorably arises between these scales. Plastic distortion of the braze matrix did not appear. Figure 10c, d shows typical fractographic SEM images of the steel and ceramic surface. The oxide layer formed on the Crofer surface can be detected in Fig. 10c, d as the very upper layer of both figures. The steel and ceramic parts revealed flat oxide layers on the surfaces. During the shear tests the maximum shear strength of 123 MPa in the entire set was achieved for this specimen.

Figure 11a, b demonstrate the digital microscope images of two corresponding halves of fractured reactive air brazed Crofer 22 APU/ $\text{Al}_2\text{O}_3$  parts at 1100 °C for 5 min after the shear strength experiment. As seen in the images the Crofer and the aluminum oxide side of the specimens expose the surfaces at the upper right half of the Crofer side and at the upper left half of the aluminum oxide sample side covered by the oxide elements of the reaction layer. These areas are noticeable on the samples as dark grey. The fracture is on the one side observable within the interfacial reaction layer at the braze filler metal–Crofer interlayer. At the lower half of the samples region Ag islands are visible. This can be recognized as white regions in the digital microscope images. Additionally, small not completely wetted areas of the ceramic are shown as grey regions in Fig. 11b. Characteristic fractographic SEM



**Fig. 10** Fracture surfaces after shear strength experiments of reactive air brazed Crofer 22 APU- $\text{Al}_2\text{O}_3$  joint brazed with Ag-4CuO filler alloy ( $T_b = 1000^\circ\text{C}$ ,  $t_d = 5$  min) **a** digital microscope image of the Crofer side, **b** corresponding aluminum oxide counterpart, **c** SEM micrograph (BSE mode) of the Crofer, **d** corresponding aluminum oxide side, **e** Characteristic SEM image of the cross-section of the steel, **f** corresponding aluminum oxide brazing compound



images of the Crofer and aluminum oxide surface are presented in Fig. 11c, d.

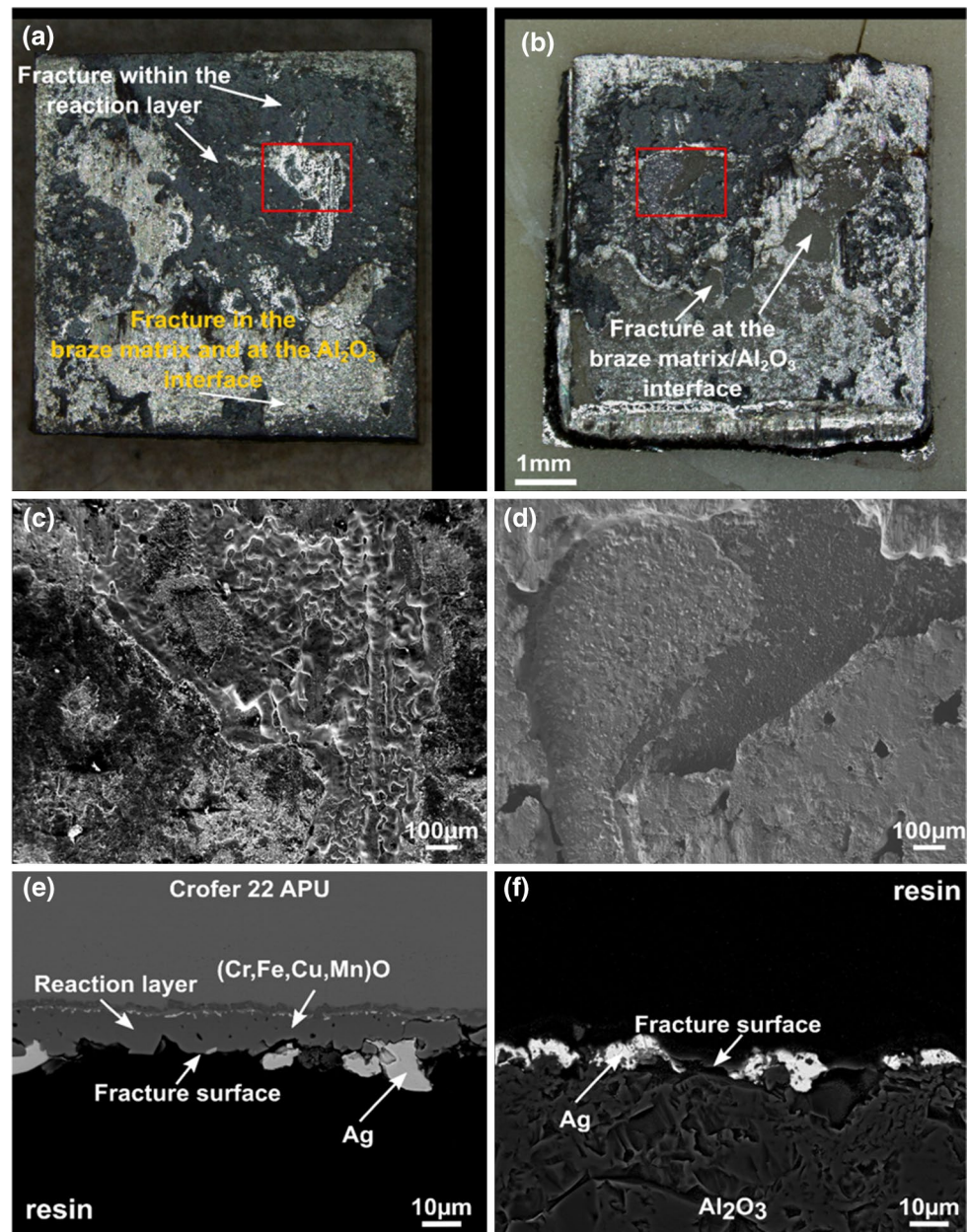
On the other side an debonding at the braze filler metal/aluminum oxide interface is visible in these images, in addition to ductile fracture of few Ag islands that remain well adhered to the ceramic faying surface. This mixed failure mode is believed to be the direct result of the wetting behavior between the silver-4 wt% copper oxide braze filler alloy and the aluminum oxide substrate. This leads to poor joint shear strength. During the shear experiments the minimum shear strength of 62 MPa in the entire set was succeeded for this specimen. The SEM micrographs show the cross-sections of the Crofer (see Fig. 11e) and the  $\text{Al}_2\text{O}_3$  (see Fig. 11f) after fracture. The mechanical failure

was perceived to be controlled by different phenomena. Mixed failure mode occurred within the interfacial reaction layer at the braze filler metal–Crofer interface and in the braze matrix or at the braze filler metal– $\text{Al}_2\text{O}_3$  interface.

## 4 Conclusions

Within this study, a brazing filler manufacturing process employing arc-PVD was utilized and investigated for the joining of metal–ceramic composites. The effect of different brazing temperatures and holding times on the interfacial microstructures and shear strength behavior were characterized for reactive air brazed Crofer 22 APU- $\text{Al}_2\text{O}_3$

**Fig. 11** Fracture surfaces after shear strength experiments of reactive air brazed Crofer 22 APU- $\text{Al}_2\text{O}_3$  joint brazed using the Ag-4CuO filler alloy ( $T_b = 1100^\circ\text{C}$ ,  $t_d = 5$  min): **a** digital microscope image of the Crofer side, **b** corresponding aluminum oxide counterpart, **c** SEM micrograph (BSE mode) of the Crofer, **d** corresponding aluminum oxide side, **e** Characteristic SEM image of the cross-section of the steel, **f** corresponding aluminum oxide brazing compound



joints. For this, the braze filler metal Ag4CuO was used. Additionally, the classification of different phases was conducted by EDS-measurements in arrangement with microhardness measurements. Discussion of the results focused on the impact of microstructural development on mechanical properties, the pore formation in the brazing seam and failure behavior of the brazed joints. The most substantial conclusions drawn from the results of the brazed joints are potted as follows:

- Coating of copper by arc-PVD on the surface of pure Ag foil was successful for the production of AgCu braze filler metals.
- The corresponding brazing seam was pores and voids free. The wetting behavior of the brazing alloy at the interface of the aluminum oxide and of the Crofer was brilliant. Compact bonding was succeeded for all samples without the occurrence of visible cracks.
- Interfacial reaction layers between the Crofer and the braze filler metal were observed. The formation and the thickness of the interfacial reaction layer with a large content of brittle reaction oxides can be inconvenient for the joint strength.
- The best shear strength results of 123 MPa was realized with a brazing temperature of  $1000^\circ\text{C}$  and a dwell time of 5 min, using the RAB.



- In many cases, the joined samples failed in the reaction layer at the braze filler metal–Crofer interface. Fracture surfaces exposed for a small number of samples a mixed failure mode within the interfacial reaction layer at the braze filler metal–Crofer interface and in the braze matrix or at the braze filler metal–Al<sub>2</sub>O<sub>3</sub> interface.

**Acknowledgements** The authors gratefully acknowledge the financial support of the German Research Foundation (DFG) within the project TI 343/147–1 (In situ investigation of the pore development during reactive air brazing of aluminum oxide ceramics).

## Compliance with ethical standards

**Conflict of interest** The authors declare that they have no conflict of interest.

## References

- Kaletsch A, Bezold A, Pfaff EM, Broeckmann C (2012) Effects of copper oxide content in the AgCuO braze alloy on microstructure and mechanical properties of reactive air brazed Ba<sub>0.5</sub>Sr<sub>0.5</sub>Co<sub>0.8</sub>Fe<sub>0.2</sub>O<sub>3</sub> δ (BSCF). *J Ceram Sci Technol* 3(2):95–104
- Kim JY, Hardy JS, Scott Weil K (2005) Effects of CuO content on the wetting behavior and mechanical properties of a Ag–CuO braze for ceramic joining. *J Am Ceram Soc* 88(9):2521–2527
- Kim JY, Weil KS (2007) Effects of brazing time and temperature on the microstructure and mechanical properties of aluminum air brazed joints. *J Am Ceram Soc* 90(12):3830–3837
- Fernie JA, Drew RAL, Knowles KM (2009) Joining of engineering ceramics. *Int Mater Rev* 54(5):283–331
- Schwartz MM (1990) *Ceramic joining*, 1st edn. ASM International, Materials Park
- Tillmann W (1992) *Aspekte des Aktivlötens nichtoxidischer Ingenieurskeramiken*. Dissertation, Lehrgebiet Werkstoffwissenschaften der RWTH Aachen
- Bobzin K, Öte M, Wiesner S, Kaletsch A, Broeckmann C (2014) Characterization of reactive air brazed ceramic/metal joints with unadapted thermal expansion behavior. *Adv Eng Mater* 16(12):1490–1497
- Bobzin K, Schläfer T, Kopp N (2011) Thermochemistry of brazing ceramics and metals in air. *Int J Mater Res* 102(8):972–976
- Nicholas MG (ed) (1990) *Joining of ceramics*. Chapman and Hall, London
- Boretius M, Lugscheider E, Tillmann W (1995) *Fügen von Hochleistungskeramik: Verfahren, Auslegung, Prüfung*. VDI-Verlag, Düsseldorf, Anwendung
- Walker CA, Hodges VC (2008) Comparing metal-ceramic brazing methods. *Weld J* 43:43–50
- Nascimento RMD, Martinelli AE, Buschinelli AJA (2003) Review Article: recent advances in metal-ceramic brazing. *Cerâmica* 49(312):178–198
- Nicholas MG (1993) Reactive wetting and brazing of ceramics. In: *Proceedings of the 4th international conference joining ceramics, glass and metal*, pp 57–67
- Schüler H (2001) *Simulation von Lötprozessen beim Metall-Keramik-Löten*. Dissertation, Technische Universität Chemnitz
- Ovenstone J, Jung JI, White JS, Edwards DD, Misture ST (2008) Phase stability of BSCF in low oxygen partial pressures. *J Solid State Chem* 181(3):576–586
- Kim JH, Yoo YC (1997) Bonding of alumina to metals with Ag–Cu–Zr brazing alloy. *J Mater Sci Lett* 16(13):1212–1215
- Weil KS, Rice JP (2005) Substrate effects on the high-temperature oxidation behavior of a gold-based braze filler metal. *Scr Mater* 52(11):1081–1085
- Kim JY, Hardy JS, Weil KS (2004) Use of aluminum in air-brazing aluminum oxide. *J Mater Res* 19(6):1717–1722
- Kozlova O, Braccini M, Voytovych R, Eustathopoulos N, Martinetti P, Devismes MF (2010) Brazing copper to alumina using reactive CuAgTi alloys. *Acta Mater* 58(4):1252–1260
- Eichler K, Solow G, Otschick P, Schaffrath W (2000) Degradation effects at sealing glasses for the SOFC. In: McEvoy AJ (ed) *Proceedings of the fourth European solid oxide fuel cell forum*, Oberrohrdorf, Switzerland. pp 899–906
- Lewinsohn CA, Singh M, Shibayama T, Hinoki T, Ando M, Katoh Y, Kohyama A (2000) Joining of silicon carbide composites for fusion energy applications. *J Nucl Mater* 283–287:1258–1261
- Erskine KM, Meier AM, Pilgrim SM (2002) Brazing perovskite ceramics with silver/copper oxide braze alloys. *J Mater Sci* 37(8):1705–1709
- Weil KS, Kim JY, Hardy JS (2005) Reactive air brazing: a novel method of sealing SOFCs and other solid-state electrochemical devices. *Electrochem Solid St* 8(2):133–136
- Weil KS, Hardy JS, Rice J, Kim J (2006) Brazing as a means of sealing ceramic membranes for use in advanced coal gasification processes. *Fuel* 85(2):156–162
- Weil KS, Kim JY, Hardy JS, Darsell JT (2006) The effect of TiO<sub>2</sub> on the wetting behavior of silver–copper oxide braze filler metals. *Scr Mater* 54(6):1071–1075
- Chen H, Li L, Kemps R, Michielsen B, Jacobs M, Snijkers F, Middelkoop V (2015) Reactive air brazing for sealing mixed ionic electronic conducting hollow fibre membranes. *Acta Mater* 88:74–82
- Weil KS, Coyle CA, Darsell JT, Xia GG, Hardy JS (2005) Effects of thermal cycling and thermal aging on the hermeticity and strength of silver–copper oxide air-brazed seals. *J Power Sources* 152:97–104
- Schüler CC, Stuck A, Beck N, Keser H, Täck U (2000) Direct silver bonding—an alternative for substrates in power semiconductor packaging. *J Mater Sci Mater Electron* 11(5):389–396
- Bobzin K, Schläfer T, Zhao L, Kopp N, Schlegel A (2010) Brazing of ceramic-to-ceramic and ceramic-to-metal joints in air. *Front Mech Eng China* 5(2):125–129
- Kim JY, Hardy JS, Weil KS (2005) Silver-copper oxide based reactive air braze for joining yttria-stabilized zirconia. *J Mater Res* 20(03):636–643
- Kim JY, Hardy JS, Weil KS (2007) Dual-atmosphere tolerance of Ag–CuO-based air braze. *Int J Hydrogen Energy* 32(16):3655–3663
- Kim JY, Weil KS, Hardy JS (2006) Wetting and mechanical characteristics of the reactive air braze for yttria-stabilized zirconia (YSZ) joining. In: Weil KS, Reimanis IE, Lewinsohn CA (eds) *Surfaces, interfaces and science of ceramic joining*. The American Ceramic Society, Westerville, pp 101–109 (**Ceramic Transactions Bd. 158**)
- Kuhn B, Wessel E, Malzbender J, Steinbrech RW, Singheiser L (2010) Effect of isothermal aging on the mechanical performance of brazed ceramic/metal joints for planar SOFC-stacks. *Int J Hydrogen Energy* 35(17):9158–9165
- Kuhn B (2009) *Bruchmechanische Untersuchung von Metall, Keramik-Verbundsystemen für die Anwendung in der Hochtemperaturbrennstoffzelle (SOFC)*. Forschungszentrum Jülich, Zentralbibliothek, Jülich, 2009 (Schriften des Forschungszentrums

- Jülich, Reihe Energie & Umwelt Bd. 50). ISBN 978-33-89336-592-0.-Dissertation, Technische Universität Clausthal. Schriften des Forschungszentrums Jülich/Reihe Energie & Umwelt Bd. 50
35. Bobzin K, Kopp N, Wiesner S (2014) Influence of filler and base material on the pore development during reactive air brazing. *Adv Eng Mater* 16(12):1456–1461
  36. Kopp N (2012) Reaktive Air Brazing - Löten von Keramik-Keramik und Keramik-Metall-Verbunden an Luft. Dissertation, RWTH-Aachen
  37. Darsell JT, Weil KS (2011) High temperature strength of YSZ joints brazed with palladium silver copper oxide filler metals. *Int J Hydrogen Energ* 36(7):4519–4524
  38. Darsell JT, Weil KS (2008) Effect of filler metal composition on the strength of yttria stabilized zirconia joints brazed with Pd–Ag–CuO<sub>x</sub>. *Metall Mater Trans A*. <https://doi.org/10.1007/s11661-008-9565-7>
  39. ThyssenKupp VDM-Metals GmbH “VDM® Crofer 22 APU”, data sheet, received: 11.10.2019, 10:51 GMT+1
  40. Ardigò MR, Perron A, Combemale L, Heintz O, Caboche G, Chevalier S (2011) Interface reactivity study between La<sub>0.6</sub>Sr<sub>0.4</sub>Co<sub>0.2</sub>Fe<sub>0.8</sub>O<sub>3-δ</sub> (LSCF) cathode material and metallic interconnect for fuel cell. *J Power Sources* 196(4):2037–2045
  41. Brylewski T (2001) Application of Fe–16Cr ferritic alloy to interconnector for a solid oxide fuel cell. *Solid State Ionics* 143(2):131–150
  42. Fergus JW (2005) Metallic interconnects for solid oxide fuel cells. *Mater Sci Eng A* 397(1–2):271–283
  43. Kadowaki T, Shiomitsu T, Matsuda E, Nakagawa H, Tsuneizumi H, Maruyama T (1993) Applicability of heat resisting alloys to the separator of planar type solid oxide fuel cell. *Solid State Ionics* 67(1–2):65–69
  44. Przybylski K, Brylewski T, Durda E, Gawel R, Kruk A (2014) Oxidation properties of the Crofer 22 APU steel coated with La<sub>0.6</sub>Sr<sub>0.4</sub>Co<sub>0.2</sub>Fe<sub>0.8</sub>O<sub>3</sub> for IT-SOFC interconnect applications. *J Therm Anal Calorim* 116(2):825–834
  45. Kyocera Fin ceramics Solution GmbH “Degussit AL23” Aluminum oxide, data sheet, received: 17.10.2019, 08:51 GMT+1
  46. Elrefaey A, Wojarski L, Janczak-Rusch J, Tillmann W (2013) Vacuum brazing titanium using thin nickel layer deposited by PVD technique. *Mater Sci Eng A* 565:180–186
  47. Tillmann W, Wojarski L, Manka M, Timmer C (2018) Eutectic high entropy alloys—a novel class of materials for brazing applications. In: Proceedings from the 7th international brazing and soldering conference (IBSC 2018), New Orleans, USA, pp 135–141
  48. Wojarski L, Tillmann W (2014) TLP brazing of aluminum to steel using PVD-deposited interlayer. *Weld World* 58(5):673–680
  49. Steffens HD, Wilden J, Möhwald K (1995) Utilization of ion plated diffusion barriers and brazing alloys for steel/titanium- and steel/aluminium-joints. *DVS-Berichte* 166:94–98
  50. Raju K, Muksin Kim S, Song KS, Yu JH, Yoon DH (2016) Joining of metal–ceramic using reactive air brazing for oxygen transport membrane applications. *Mater Des* 109:233–241
  51. Poenicke A, Arnold S, Schilm J, Kusnezoff M, Michaelis A (2012) In: Gourley R (ed) Brazing and soldering: proceedings of the 5th International brazing and soldering conference 22–25 Apr 2012, Red Rock Casino Resort Spa, Las Vegas, Nevada. ASM International, Materials Park, pp 450–457
  52. Li C, Kuhn B, Brandenburg J, Beck T, Singheiser L, Bobzin K, Bagciyan N, Kopp N (2012) Improving contour accuracy and strength of reactive air brazed (RAB) ceramic/metal joints by controlling interface microstructure. *Adv Eng Mater* 14(6):394–399
  53. Magdefrau NJ, Chen L, Sun EY, Aindow M (2013) Effects of alloy heat treatment on oxidation kinetics and scale morphology for Crofer 22 APU. *J Power Sources* 241:756–767
  54. Raju K, Kim S, Seong YH, Yoon DH (2019) Effects of reactive air brazing parameters on the interfacial microstructure and shear strength of GDC–LSM/Crofer 22 APU joints. *J Korean Ceram Soc* 56(4):394–398
  55. Li C (2013) Mechanical behavior and microstructure of reactive-air-brazed metal/ceramic joints. PhD Thesis, RWTH Aachen University

**Publisher's Note** Springer Nature remains neutral with regard to jurisdictional claims in published maps and institutional affiliations.